GKSS
FORSCHUNGSZENTRUM
in der HELMHOLTZ GEMEINSCHAFT

An extended Chaboche viscoplastic law at finite strains and its numerical implementation

Authors:
W. Brocks
Ruocheng Lin

ISSN 0344-9629

GKSS 2003/20

GKSS 2003/20

An extended Chaboche viscoplastic law at finite strains and its numerical implementation

Authors:

W. Brocks
Ruocheng Lin
(Institute for Materials Research)

GKSS-Forschungszentrum Geesthacht GmbH • Geesthacht • 2003

Die Berichte der GKSS werden kostenlos abgegeben.
The delivery of the GKSS reports is free of charge.

Anforderungen/Requests:

GKSS-Forschungszentrum Geesthacht GmbH
Bibliothek/Library
Postfach 11 60
D-21494 Geesthacht
Germany
Fax.: (49) 04152/871717

ISSN 0344-9629

GKSS-Forschungszentrum Geesthacht GmbH · Telefon (04152)87-0
Max-Planck-Straße · D-21502 Geesthacht / Postfach 11 60 · D-21494 Geesthacht

GKSS 2003/20

An extended Chaboche viscoplastic law at finite strains and its numerical implementation

Wolfgang Brocks and Ruocheng Lin

29 pages with 5 figures and 1 table

Abstract

Many applications have proven that the Chaboche viscoplastic laws can characterize constitutive responses of metals very well. But, almost all of the Chaboche material laws are mathematically formulated for infinitesimal deformations. This mathematical limitation obstructs the application of these laws in many cases, for example, in the simulations of metal forming. In the present work a Chaboche viscoplastic law is extended to finite strain form based on an internal dissipation inequality. Therefore, this extension is consistent with the second law of thermodynamics. The obtained finite strain law has a concise form. In order to numerically investigate the extended viscoplastic law, a numerical algorithm for the finite element implementation of this law is formulated and several numerical examples are presented. These numerical examples prove that the extended viscoplastic law is effective and the numerical implementation is correct.

Ein verallgemeinertes Chaboche-Viskoplastizitätsgesetz bei finiten Dehnungen und seine numerische Implementierung

Zusammenfassung

Viele Anwendungen haben bewiesen, dass die viskoplastischen Stoffgesetze vom Chaboche-Typ konstitutive Antworten von Metallen sehr gut beschreiben können. Aber fast alle Chaboche-Materialgesetze werden mathematisch für infinitesimale Verformungen formuliert. Diese mathematische Beschränkung verhindert die Anwendung solcher Gesetze in vielen Fällen, z.B. in der Simulation von Metallumformung. In der vorliegenden Arbeit wird ein Chaboche-Viskoplastizitätsgesetz auf der Basis einer Ungleichung der inneren Dissipation für finite Dehnungen verallgemeinert. Deshalb ist diese Verallgemeinerung mit dem zweiten Hauptsatz der Thermodynamik konsistent. Das erhaltene Gesetz bei finiten Dehnungen besitzt eine übersichtliche Form. Um das verallgemeinerte Viskoplastizitätsgesetz numerisch zu untersuchen, wird ein numerischer Algorithmus für die Finite-Elemente-Implementierung dieses Gesetzes formuliert, und es werden einige numerische Beispiele präsentiert. Diese numerischen Beispiele beweisen, dass das verallgemeinerte Viskoplastizitätsgesetz effektiv und die numerische Implementierung korrekt sind.

Manuskripteingang in TDB: 15. August 2003

Contents

1 Introduction 1

2 A Chaboche viscoplastic law at small deformations 2

3 The Extended viscoplastic law at finite strains 6

4 Algorithm aspects 11
4.1 Local discrete evolution equations 11
4.2 Return mapping algorithm in principal stresses 12
4.3 Consistent elastoplastic tangent moduli 14

5 Numerical examples 17
5.1 Elastic stress response of a closed deformation process 17
5.2 Comparison with experimental observation at cyclic uniaxial loading 18
5.3 Stress response at simple shear 19
5.4 Mechanical response of an axisymmetric billet in upsetting 19

6 Conclusions 21

1 Introduction

Many applications have proven that the Chaboche viscoplastic laws can characterize constitutive responses of many metals very well, see e.g. Chaboche (1989) and Lemaitre and Chaboche (1990). But, almost all of the Chaboche laws are formulated in the context of infinitesimal deformations, see e.g. Chaboche (1977, 1989, 1993a,b, 1997), Chaboche and Jung (1998), Chaboche and Rousselier (1983a,b) as well as Lemaitre and Chaboche (1990). This assumption hinders the application of these laws to problems with finite deformations, for example, to simulation of metal forming processes and description of mechanical responses of metal structures at finite deformations. In order to exploit the advantages of the Chaboche laws for finite deformation problems it is necessary to extend the classical Chaboche laws to the framework of finite deformation.

The finite strain plastic and viscoplastic theories are usually based on conventional objective stress rates and hypoelastic laws. This type of formulation is also extensively applied in the commercial general-purpose finite element programs, for example in ABAQUS (1998). By this approach, one can also reformulate the Chaboche laws in the finite strain form. But, it has been shown that the hypoelastic equations related to the conventional stress rates are not consistent with elasticity and cause spurious constitutive responses in deformation processes with finite rotations (Lin, 2002b, 2003). Simo and Pister (1984) suggested that the hypoelastic formulation should be replaced by the hyperelastic formulation for establishing a finite strain inelastic law. In recent years several finite strain plastic and viscoplastic theories based on the latter formulation have been presented. See, for example, the works of Simo (1992), Simo and Miehe (1992) as well as Miehe (1998). In the present contribution the extension of an infinitesimal Chaboche viscoplastic law is based on the hyperelastic formulation. In this aspect the present formulation is identical to the above three hyperelasticity-based plastic theories. Differing from them the present finite strain viscoplastic theory is based on a new and more concise dissipation inequality. The obtained finite strain law can be easily numerically implemented and experimentally identified. In this work some numerical examples with finite deformations are given to justify the effectivity of the extended law and numerical implementation.

2 A Chaboche viscoplastic law at small deformations

To motivate the extension of the Chaboche viscoplastic law to finite strain form it is summarized in this chapter. This summary stems mainly from the works presented in Chaboche (1993a,b), Chaboche and Jung (1998), Lemaitre and Chaboche (1990). See also Arzt et al. (1999). This viscoplastic law is based on the phenomenological Bingham model (see Fig. 2.1). It can be easily seen that the plastic unit and the viscous unit correspond to a unique inelastic strain. In the viscoplastic laws based on this phenomenological model the effects related to two types of inelastic deformations, e.g. the hardening due to deformation (strain-hardening) and the hardening due to time (time-hardening), are usually treated in combined ways. In this sense this class of viscoplastic laws is usually called *unified* viscoplastic law.

The following additive decomposition of total strain $\boldsymbol{\varepsilon}$ is assumed, i.e.

$$\boldsymbol{\varepsilon} = \boldsymbol{\varepsilon}^e + \boldsymbol{\varepsilon}^p \,, \tag{2.1}$$

where $\boldsymbol{\varepsilon}^e$ is the linear elastic strain and $\boldsymbol{\varepsilon}^p$ is the viscoplastic strain. This additive decomposition is consistent with the experimental observation that for most metals the elastic behavior is not affected by the magnitude of viscoplastic strain. The total strain is specified by the partial derivative of displacement $\boldsymbol{u}$ with respect to spatial position vector $\boldsymbol{x}$; i.e. $\boldsymbol{\varepsilon} = \frac{1}{2}\left[\frac{\partial \boldsymbol{u}}{\partial \boldsymbol{x}} + (\frac{\partial \boldsymbol{u}}{\partial \boldsymbol{x}})^{\mathrm{T}}\right]$. In general, both the elastic strain and the viscoplastic strain can be considered as internal variables. But, only one of them is independent because of equation (2.1). In this viscoplastic law the viscoplastic strain is chosen as an independent internal variables. Isotropic and kinematic hardening are included. In order to treat both types of hardening two strain-like internal variables: the scalar p and the rank-two strain-like tensor $\boldsymbol{\xi}$ are introduced. The former is used to characterize isotropic hardening and can be chosen, as a specific case, as $p = \varepsilon^p = \int_0^t \left(\frac{2}{3}\dot{\boldsymbol{\varepsilon}}^p : \dot{\boldsymbol{\varepsilon}}^p\right)^{1/2} \mathrm{d}\tau$, with ε^p being the accumulated plastic strain. The latter is assumed to be work-conjugate to a stress-like internal variable: the back stress $\boldsymbol{\alpha}$ and is used to characterize kinematic hardening.

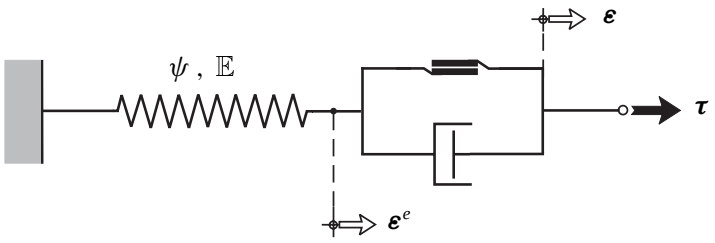

Figure 2.1: Bingham phenomenological model.

In this constitutive theory it is assumed that there are two types of potential functions: the free energy function Ψ described in the strain space and the dissipation potential function Φ described in the stress space. Further, the free energy (per unit reference volume) is assumed to be decoupled and is formulated as (see e.g. Lemaitre and Chaboche (1990), p. 312)

$$\Psi = \psi_e(\boldsymbol{\varepsilon}^e) + g(\boldsymbol{\xi}) + \ h(p) \ , \tag{2.2}$$

where ψ_e and g are the elastic free energy and the kinematic hardening function defined respectively as

$$\psi_e(\boldsymbol{\varepsilon}^e) = \tfrac{1}{2}\,\boldsymbol{\varepsilon}^e : \mathbb{C} : \boldsymbol{\varepsilon}^e \ , \qquad g(\boldsymbol{\xi}) = \tfrac{1}{3} C\,\boldsymbol{\xi} : \boldsymbol{\xi} \ . \tag{2.3}$$

Here, $\mathbb{C}$ is an isotropic rank-four elastic tensor defined by $\mathbb{C} = \lambda \mathbf{1} \otimes \mathbf{1} + 2\mu\mathbb{I}$, with λ, μ being the Lamé constants. $\mathbf{1}$ and $\mathbb{I}$ denoting the rank-two and the rank-four identity tensor, respectively. C is a material constant. The isotropic hardening function h is chosen as

$$h(p) = Q\,\{p - [1 - \exp(-bp)]/b\} \ , \tag{2.4}$$

where Q and b are material constants. The former stands for the asymptotic value of the isotropic hardening function. From the above three free energy functions we get the corresponding stress-like counterparts

$$\boldsymbol{\sigma} = \frac{\partial \Psi}{\partial\, \boldsymbol{\varepsilon}^e} = \mathbb{C} : \boldsymbol{\varepsilon}^e \ , \qquad \boldsymbol{\alpha} = \frac{\partial \Psi}{\partial\, \boldsymbol{\xi}} = \frac{2}{3} C\,\boldsymbol{\xi} \ , \qquad R = \frac{\partial \Psi}{\partial p} = Q\,\{1 - \exp(-bp)\} \ . \tag{2.5}$$

In order to form the evolution equations of the internal variables $\boldsymbol{\varepsilon}^p$, p and $\boldsymbol{\xi}$, the concept of dissipation potential is applied and it is assumed that the normality rule is applicable, see Lemaitre and Chaboche (1990), pp. 278–280. In this viscoplastic law the dissipation potential function Φ is assumed to consist of two decoupled parts: the plastic potential function ϕ_p and the recovery potential function ϕ_r, i.e.

$$\Phi = \phi_p(\boldsymbol{\sigma}, \boldsymbol{\alpha}, R) + \phi_r(\boldsymbol{\alpha}) \ , \tag{2.6}$$

with ϕ_p and ϕ_r defined by

$$\phi_p(\boldsymbol{\sigma}, \boldsymbol{\alpha}, R) = \ f(\boldsymbol{\sigma}, \boldsymbol{\alpha}, R) + \tfrac{1}{2}\tfrac{1}{a}\gamma(p) J_2^2(\boldsymbol{\alpha}) \ , \qquad \phi_r(\boldsymbol{\alpha}) = d\, J_2(\boldsymbol{\alpha})/C \ . \tag{2.7}$$

Where a, d and C are material constants. Function $J_2(\boldsymbol{\alpha})$ is defined by

$$J_2(\boldsymbol{\alpha}) = \sqrt{\tfrac{3}{2}\,\boldsymbol{\alpha} : \boldsymbol{\alpha}} \ . \tag{2.8}$$

$f(\boldsymbol{\sigma}, \boldsymbol{\alpha}, R)$ is the yield function

$$f(\boldsymbol{\sigma}, \boldsymbol{\alpha}, R) = J_2(\boldsymbol{s} - \boldsymbol{\alpha}) - k - R = \sqrt{\tfrac{3}{2}(\boldsymbol{s} - \boldsymbol{\alpha}) : (\boldsymbol{s} - \boldsymbol{\alpha})} - k - R \ , \tag{2.9}$$

with $\boldsymbol{s}$ being the deviator of the stress tensor $\boldsymbol{\sigma}$, i.e. $\boldsymbol{s} = \boldsymbol{\sigma} - \frac{1}{3}\,\mathrm{tr}\,\boldsymbol{\sigma}\ \mathbf{1}$. In equation (2.9) k stands for the yield strength at zero plastic strain. It should be noted here that in equation $(2.7)_1$ the

accumulated plastic strain p is only a parameter of the plastic potential function ϕ_p (see Lemaitre and Chaboche (1990), pp. 279), although it is the argument of the function of the relaxation term $\gamma(p)$. The function $\gamma(p)$ is defined as

$$\gamma(p) = \gamma_\infty + (1 - \gamma_\infty)\exp(-\omega p) \ , \tag{2.10}$$

where γ_∞ and ω are material constants.

By extending the standard normality rule the evolution equations

$$\begin{aligned} \dot{\boldsymbol{\varepsilon}}^p &= \dot{\lambda}_p \frac{\partial \phi_p}{\partial \boldsymbol{\sigma}} + \dot{\lambda}_s \frac{\partial \phi_r}{\partial \boldsymbol{\sigma}} = \dot{\lambda}_p \frac{\partial \phi_p}{\partial \boldsymbol{\sigma}} \ , \\ -\dot{\boldsymbol{\xi}} &= \dot{\lambda}_p \frac{\partial \phi_p}{\partial \boldsymbol{\alpha}} + \dot{\lambda}_s \frac{\partial \phi_r}{\partial \boldsymbol{\alpha}} \ , \\ -\dot{p} &= \dot{\lambda}_p \frac{\partial \phi_p}{\partial R} + \dot{\lambda}_s \frac{\partial \phi_r}{\partial R} = \dot{\lambda}_p \frac{\partial \phi_p}{\partial R} \ , \end{aligned} \tag{2.11}$$

are obtained. In these formulations the independent plastic and static recovery multipliers $\dot{\lambda}_p$ and $\dot{\lambda}_s$ are applied. In the case of pure plasticity the plastic multiplier can be determined by the consistency condition $\dot{f}(\boldsymbol{\sigma}, \boldsymbol{\alpha}, R) = 0$. This condition means that in loading processes the stress always lies on the current yield surface. In the case of unified viscoplasticity the stress can lie outside the yield envelope. Therefore, the consistency condition is no more applicable. In this constitutive law the plastic multiplier is chosen as

$$\dot{\lambda}_p = \left[\frac{\langle f(\boldsymbol{\sigma}, \boldsymbol{\alpha}, R) \rangle}{K} \right]^m \ , \tag{2.12}$$

with K being the coefficient of resistance, m the hardening exponent. Where $\langle \cdot \rangle$ denotes the Macauley bracket with definition $\langle y \rangle = y$ if $y > 0$, and $\langle y \rangle = 0$ if $y \leq 0$. The static recovery multiplier $\dot{\lambda}_s$ is also given as a power function

$$\dot{\lambda}_s = \left[\frac{J_2(\boldsymbol{\alpha})}{a} \right]^r \ , \tag{2.13}$$

where r is a material constant.

Application of equations (2.7)–(2.9) in equation (2.11) gives the evolution equations

$$\begin{aligned} \dot{\boldsymbol{\varepsilon}}^p &= \frac{3}{2} \frac{\boldsymbol{s} - \boldsymbol{\alpha}}{J_2(\boldsymbol{s} - \boldsymbol{\alpha})} \dot{\lambda}_p \ , \\ \dot{\boldsymbol{\xi}} &= \frac{3}{2} \frac{\boldsymbol{s} - \boldsymbol{\alpha}}{J_2(\boldsymbol{s} - \boldsymbol{\alpha})} \dot{\lambda}_p - \frac{3\gamma(p)\boldsymbol{\alpha}}{2a} \dot{\lambda}_p - \frac{3d}{2C} \frac{\boldsymbol{\alpha}}{J_2(\boldsymbol{\alpha})} \dot{\lambda}_s \\ \dot{p} &= \dot{\lambda}_p = \sqrt{\tfrac{2}{3} \dot{\boldsymbol{\varepsilon}}^p : \dot{\boldsymbol{\varepsilon}}^p} \ . \end{aligned} \tag{2.14}$$

After getting the strain-like internal variables $\boldsymbol{\varepsilon}^p$, $\boldsymbol{\xi}$ and p by integrating these evolution equations we can compute the stress-like variables $\boldsymbol{\sigma}$, $\boldsymbol{\alpha}$ and R by virtue of equations (2.1) and (2.5). In fact, one can directly formulate the evolution equations of the stress-like internal variables $\boldsymbol{\alpha}$ and R by combining $(2.5)_{2,3}$ with $(2.14)_{2,3}$; i.e.

$$\dot{\boldsymbol{\alpha}} = \left[\frac{\boldsymbol{s} - \boldsymbol{\alpha}}{J_2(\boldsymbol{s} - \boldsymbol{\alpha})} - \frac{\gamma(p)\,\boldsymbol{\alpha}}{a} \right] C \dot{\lambda}_p - \frac{d\,\boldsymbol{\alpha}}{J_2(\boldsymbol{\alpha})} \dot{\lambda}_s \ , \qquad \dot{R} = b(Q - R)\dot{\lambda}_p \ . \tag{2.15}$$

Therefore, we can obtain $\boldsymbol{\alpha}$ and R directly by integrating the evolution equations in (2.15).

Obviously, this constitutive law can be applied only in processes with infinitesimal deformations. Some mathematical characteristics, e.g. the time derivatives $\dot{\boldsymbol{\varepsilon}}^p$, $\dot{\boldsymbol{\alpha}}$, confine the constitutive law to infinitesimal range. Since many metal structures, for example, metal plates and shells usually work in finite deformation states and finite deformations always arise in metal forming, it is necessary to extend the Chaboche law to finite deformation form, so that the advantages of this law can be exploited at finite deformations. In the next chapter an extension of this viscoplastic law will be presented based on an internal dissipation inequality.

3 The Extended viscoplastic law at finite strains

For the extension of the Chaboche viscoplastic law we depart from the standard assumption for finite strain inelastic problems: the multiplicative decomposition of the deformation gradient $\boldsymbol{F}$ into an elastic and an inelastic deformation gradient $\boldsymbol{F}^e$ and $\boldsymbol{F}^p$; i.e.

$$\boldsymbol{F} = \boldsymbol{F}^e \boldsymbol{F}^p \, . \tag{3.1}$$

About the micromechanical expositions of this decomposition and the consistency of the decomposition with plastic flow in metal plasticity we refer to Asaro (1979, 1983) and Asaro and Rice (1977). From the total deformation gradient we can express the left Cauchy-Green tensor $\boldsymbol{b}$ and the spatial logarithmic stain $\boldsymbol{h}$ as

$$\boldsymbol{b} = \boldsymbol{F}\boldsymbol{F}^{\mathrm{T}} = \sum_{A=1}^{3} \chi_A \boldsymbol{n}_A \otimes \boldsymbol{n}_A \, , \qquad \boldsymbol{h} = \frac{1}{2} \ln \boldsymbol{b} = \frac{1}{2} \sum_{A=1}^{3} \ln \chi_A \boldsymbol{n}_A \otimes \boldsymbol{n}_A \, . \tag{3.2}$$

Where χ_A denote the eigenvalues of $\boldsymbol{b}$, while $\boldsymbol{n}_A$, with $\|\boldsymbol{n}_A\| = 1$, stand for the corresponding eigenvectors. In the following the eigenvalues of $\boldsymbol{h}$ are also denoted $h_A = \frac{1}{2} \ln \chi_A$. In the same way, we can define the elastic left Cauchy-Green tensor $\boldsymbol{b}^e$ and the elastic logarithmic strain $\boldsymbol{h}^e$ from the elastic deformation gradient; i.e.

$$\boldsymbol{b}^e = \boldsymbol{F}^e \boldsymbol{F}^{e\mathrm{T}} = \sum_{A=1}^{3} \chi_A^e \boldsymbol{n}_A^e \otimes \boldsymbol{n}_A^e \, , \qquad \boldsymbol{h}^e = \frac{1}{2} \ln \boldsymbol{b}^e = \frac{1}{2} \sum_{A=1}^{3} \ln \chi_A^e \boldsymbol{n}_A^e \otimes \boldsymbol{n}_A^e \, . \tag{3.3}$$

Here, χ_A^e are the eigenvalues of $\boldsymbol{b}^e$, while $\boldsymbol{n}_A^e$ denote the corresponding orthonormal eigenvectors. The eigenvalues of $\boldsymbol{h}^e$ are also denoted $h_A^e = \frac{1}{2} \ln \chi_A^e$ hereafter.

It has been proven by Lin (2002a) that for the finite strain inelastic problems with initial isotropy there is the internal dissipation inequality

$$\mathcal{D}_{\mathrm{int}} = \boldsymbol{\tau} : \left(\mathring{\boldsymbol{h}}^{\log} - \mathring{\boldsymbol{h}}^{e} \right) \geq 0 \, , \tag{3.4}$$

where $\mathcal{D}_{\mathrm{int}}$ is the energy dissipation per unit reference volume and unit time caused by inelastic deformation. $\boldsymbol{\tau}$ is the Kirchhoff stress, $\mathring{\boldsymbol{h}}^{\log}$ denotes the logarithmic corotational rate of the logarithmic strain $\boldsymbol{h}$. About a detailed account of the logarithmic corotational rates of rank-two objective tensors the works of Xiao et al. (1998a,b) can be consulted. The corotational rate $\mathring{\boldsymbol{h}}^{e}$ is coaxial to the elastic logarithmic strain $\boldsymbol{h}^e$. In the following this corotational rate is called elastic corotational rate. In comparison with two extensively used dissipation inequalities: Simo's and Lion's inequalities (see e.g. Simo (1992), Simo and Miehe (1992) and Lion (1997)) , this inequality has a

concise mathematical structure. This advantage can simplify the numerical implementation and the experimental identification of the constitutive laws based on this inequality. The inequality (3.4) provides us a dissipation-conjugate pair: the driving force $\boldsymbol{\tau}$ and the dissipation term $\overset{\circ}{\boldsymbol{h}}{}^{\log} - \overset{\circ}{\boldsymbol{h}}{}^{e}$, which can be used to construct inelastic constitutive laws in the frame of thermodynamics.

Now, we return to the extension of the small strain Chaboche viscoplastic law. As well known, for finite strain inelastic problems the constitutive laws can be formulated in the current configuration, the reference configuration and in the (released) intermediate configuration. But, the constitutive responses in the current configuration are usually required, therefore, we carry out the extension directly in the current configuration. For the extension we assume that the mathematical structures of the free energy and dissipation potential functions in equations (2.2) and (2.6) can be inherited at finite strains. We change the definitions of the arguments in these potential functions and reformulate the evolution equations of the internal variables so that the extended viscoplastic law satisfies the requirement of material frame indifference and is suitable for modeling finite strain viscoplastic problems. It should be noted that because of the requirement of material frame indifference all (independent and dependent) variables must be objective. According to the argument of Simo (1998), pp. 331–332, the extended potential functions must be isotropic with respect to their arguments. According to the above assumptions the total free energy function Ψ has the formulation (2.2), with the elastic stored energy ψ_e redefined by Hencky's formulation; i.e.

$$\psi_e(\boldsymbol{h}^e) = \tfrac{1}{2}\boldsymbol{h}^e : \mathbb{C} : \boldsymbol{h}^e \ . \tag{3.5}$$

For the free energies contributed by kinematic and isotropic hardenings we use here the same notations $\boldsymbol{\xi}$ and p for the arguments as in equations (2.2) and (2.4), but the definitions of the arguments are changed. Here, $\boldsymbol{\xi}$ is an objective and spatially described rank-two tensor. Although p still denotes the accumulated plastic strain, it is defined here by the following formulation

$$p = \int_0^t \sqrt{\frac{2}{3}\left(\overset{\circ}{\boldsymbol{h}}{}^{\log} - \overset{\circ}{\boldsymbol{h}}{}^{e}\right) : \left(\overset{\circ}{\boldsymbol{h}}{}^{\log} - \overset{\circ}{\boldsymbol{h}}{}^{e}\right)}\ \mathrm{d}\tau \ . \tag{3.6}$$

The Kirchhoff stress $\boldsymbol{\tau}$ can be expressed as

$$\boldsymbol{\tau} = \frac{\partial \Psi}{\partial \boldsymbol{h}^e} = \mathbb{C} : \boldsymbol{h}^e \ . \tag{3.7}$$

Here, we want to note that $\boldsymbol{\tau}$ and $\boldsymbol{h}^e$ are coaxial because of the isotropic elastic free energy function (3.5). For the computation of the stress-like internal variables $\boldsymbol{\alpha}$ and R the formulations $(2.5)_{2,3}$ are still applicable.

In the extended constitutive setting the mathematical structures of the dissipation potential functions, see equations (2.6)–(2.10), are also preserved. A small modification arises in the yield function f. Here, we use the Kirchhoff stress $\boldsymbol{\tau}$ to replace the original stress tensor $\boldsymbol{\sigma}$. Equation (2.9) is then reformulated as

$$f(\boldsymbol{\tau}, \boldsymbol{\alpha}, R) = J_2(\boldsymbol{s} - \boldsymbol{\alpha}) - k - R = \sqrt{\tfrac{3}{2}(\boldsymbol{s} - \boldsymbol{\alpha}) : (\boldsymbol{s} - \boldsymbol{\alpha})} - k - R \ , \tag{3.8}$$

with the deviatoric tensor $\boldsymbol{s}$ defined by $\boldsymbol{s} = \boldsymbol{\tau} - \frac{1}{3}\operatorname{tr}\boldsymbol{\tau}\,\mathbf{1}$. Here, it should be noted that by frame invariance the yield function f must be an isotropic function of the arguments $\boldsymbol{\tau}$, $\boldsymbol{\alpha}$ and R, and can only depend on the principal values of the first two tensorial arguments. The same argument can be found in Simo (1992) and Simo (1998), pp. 331–332.

By application of the dissipation-conjugate relation between $\boldsymbol{\tau}$ and $\mathring{\boldsymbol{h}}^{\log} - \mathring{\boldsymbol{h}}^{e}$ at isotropic elasticity and recalling the isotropic behavior of the dissipation potentials, we can trivially extend the evolution equation $(2.11)_1$ to the finite strain form

$$\mathring{\boldsymbol{h}}^{\log} - \mathring{\boldsymbol{h}}^{e} = \dot{\lambda}_p \frac{\partial \phi_p}{\partial\, \boldsymbol{\tau}} + \dot{\lambda}_s \frac{\partial \phi_r}{\partial\, \boldsymbol{\tau}} = \dot{\lambda}_p \frac{\partial \phi_p}{\partial\, \boldsymbol{\tau}} \,. \tag{3.9}$$

For the spatially described objective tensor $\boldsymbol{\xi}$ we postulate the evolution equation

$$-\mathring{\boldsymbol{\xi}} = \dot{\lambda}_p \frac{\partial \phi_p}{\partial \boldsymbol{\alpha}} + \dot{\lambda}_s \frac{\partial \phi_r}{\partial \boldsymbol{\alpha}} \,, \tag{3.10}$$

with $\mathring{\boldsymbol{\xi}}$ being the objective corotational rate coaxial to $\boldsymbol{\xi}$. The evolution equation of p is identical to equation $(2.11)_3$. In these evolution equations the multipliers $\dot{\lambda}_p$ and $\dot{\lambda}_s$ are assumed to keep their definitions at small strains, only with the involved yield function f defined by (3.8). With these new formulations in hand we can extend the formulations in (2.14) to the forms

$$\begin{aligned}
&\mathring{\boldsymbol{h}}^{\log} - \mathring{\boldsymbol{h}}^{e} = \frac{3}{2}\frac{\boldsymbol{s}-\boldsymbol{\alpha}}{J_2(\boldsymbol{s}-\boldsymbol{\alpha})}\dot{\lambda}_p \,, \\
&\mathring{\boldsymbol{\xi}} = \frac{3}{2}\frac{\boldsymbol{s}-\boldsymbol{\alpha}}{J_2(\boldsymbol{s}-\boldsymbol{\alpha})}\dot{\lambda}_p - \frac{3\gamma(p)\boldsymbol{\alpha}}{2a}\dot{\lambda}_p - \frac{3d}{2C}\frac{\boldsymbol{\alpha}}{J_2(\boldsymbol{\alpha})}\dot{\lambda}_s \,, \\
&\dot{p} = \dot{\lambda}_p = \sqrt{\frac{2}{3}\left(\mathring{\boldsymbol{h}}^{\log} - \mathring{\boldsymbol{h}}^{e}\right) : \left(\mathring{\boldsymbol{h}}^{\log} - \mathring{\boldsymbol{h}}^{e}\right)} \,.
\end{aligned} \tag{3.11}$$

Taking the same procedure of formulating equation (2.15), we get the evolution equations for the stress-like internal variables $\boldsymbol{\alpha}$ and R at finite strains; i.e.

$$\mathring{\boldsymbol{\alpha}} = \left[\frac{\boldsymbol{s}-\boldsymbol{\alpha}}{J_2(\boldsymbol{s}-\boldsymbol{\alpha})} - \frac{\gamma(p)\,\boldsymbol{\alpha}}{a}\right] C\dot{\lambda}_p - \frac{d\,\boldsymbol{\alpha}}{J_2(\boldsymbol{\alpha})}\dot{\lambda}_s \,, \qquad \dot{R} = b(Q-R)\dot{\lambda}_p \,. \tag{3.12}$$

Remark 3.1. In the present constitutive setting the coaxiality of the stress deviator $\boldsymbol{s}$ and the back stress $\boldsymbol{\alpha}$ (or the strain-like internal variable $\boldsymbol{\xi}$) is implicitly included. This coaxiality means that the back stress $\boldsymbol{\alpha}$ and the stress $\boldsymbol{s}$ (i.e. $\boldsymbol{\tau}$) evolve in phase. In some finite multiplicative plastic theories, see e.g. Simo (1992) and Simo (1998), pp. 400–401, the same coaxiality has been exploited. It can be easily seen that at infinitesimal strains the present finite viscoplastic law reduces automatically to the recorded Chaboche law.

Remark 3.2. From equations (3.7), $(3.11)_1$ and recalling Remark 3.1, we know that $\mathring{\boldsymbol{h}}^{\log}$ and $\mathring{\boldsymbol{h}}^{e}$ are coaxial. This coaxiality implies that the additive decomposition of the logarithmic strain $\boldsymbol{h} = \boldsymbol{h}^{e} + \boldsymbol{h}^{p}$ is equivalent to the multiplicative decomposition of the deformation gradient $\boldsymbol{F} = \boldsymbol{F}^{e}\boldsymbol{F}^{p}$, where $\boldsymbol{h}^{p}$

Table 3.1: Extended Chaboche viscoplastic law.

Free energy functions:

$$\Psi = \psi_e(\boldsymbol{h}^e) + g(\boldsymbol{\xi}) + h(p) \ ,$$

$$\psi_e(\boldsymbol{h}^e) = \tfrac{1}{2}\boldsymbol{h}^e : \mathbb{C} : \boldsymbol{h}^e \ , \qquad g(\boldsymbol{\xi}) = \tfrac{1}{3}C\,\boldsymbol{\xi} : \boldsymbol{\xi} \ , \qquad h(p) = Q\,\{p - [1 - \exp(-bp)]/b\}$$

Kirchhoff stress and stress-like internal variables:

$$\boldsymbol{\tau} = \frac{\partial \Psi}{\partial \boldsymbol{h}^e} = \mathbb{C} : \boldsymbol{h}^e \ , \qquad \boldsymbol{\alpha} = \frac{\partial \Psi}{\partial\, \boldsymbol{\xi}} = \frac{2}{3} C\,\boldsymbol{\xi} \ , \qquad R = \frac{\partial \Psi}{\partial p} = Q\,\{1 - \exp(-bp)\}$$

Potential functions:

$$\Phi = \phi_p(\boldsymbol{\tau}, \boldsymbol{\alpha}, R) + \phi_r(\boldsymbol{\alpha}) \ ,$$

$$\phi_p(\boldsymbol{\tau}, \boldsymbol{\alpha}, R) = f(\boldsymbol{\tau}, \boldsymbol{\alpha}, R) + \tfrac{1}{2}\tfrac{1}{a}\gamma(p)\, J_2^2(\boldsymbol{\alpha}) \ , \qquad \phi_r(\boldsymbol{\alpha}) = d\, J_2(\boldsymbol{\alpha})/C \ ,$$

with

$$f(\boldsymbol{\tau}, \boldsymbol{\alpha}, R) = J_2(\boldsymbol{s} - \boldsymbol{\alpha}) - k - R = \sqrt{\tfrac{3}{2}(\boldsymbol{s} - \boldsymbol{\alpha}) : (\boldsymbol{s} - \boldsymbol{\alpha})} - k - R \ ,$$

$$\gamma(p) = \gamma_\infty + (1 - \gamma_\infty)\exp(-\omega p) \ , \qquad J_2(\boldsymbol{\alpha}) = \sqrt{\tfrac{3}{2}\,\boldsymbol{\alpha} : \boldsymbol{\alpha}} \ , \qquad \boldsymbol{s} = \boldsymbol{\tau} - \tfrac{1}{3}\operatorname{tr}\boldsymbol{\tau}\,\mathbf{1}$$

Evolution equations of strain-like internal variables:

$$\mathring{\boldsymbol{h}}^{\log} - \mathring{\boldsymbol{h}}^e = \dot\lambda_p \frac{\partial \phi_p}{\partial\, \boldsymbol{\tau}} = \frac{3}{2}\frac{\boldsymbol{s} - \boldsymbol{\alpha}}{J_2(\boldsymbol{s} - \boldsymbol{\alpha})}\dot\lambda_p \ ,$$

$$\mathring{\boldsymbol{\xi}} = -\dot\lambda_p \frac{\partial \phi_p}{\partial \boldsymbol{\alpha}} - \dot\lambda_s \frac{\partial \phi_r}{\partial \boldsymbol{\alpha}} = \frac{3}{2}\frac{\boldsymbol{s} - \boldsymbol{\alpha}}{J_2(\boldsymbol{s} - \boldsymbol{\alpha})}\dot\lambda_p - \frac{3\gamma(p)\boldsymbol{\alpha}}{2a}\dot\lambda_p - \frac{3d}{2C}\frac{\boldsymbol{\alpha}}{J_2(\boldsymbol{\alpha})}\dot\lambda_s \ ,$$

$$\dot p = -\dot\lambda_p \frac{\partial \phi_p}{\partial R} = \sqrt{\frac{2}{3}\left(\mathring{\boldsymbol{h}}^{\log} - \mathring{\boldsymbol{h}}^e\right) : \left(\mathring{\boldsymbol{h}}^{\log} - \mathring{\boldsymbol{h}}^e\right)} = \dot\lambda_p \ ,$$

with

$$\dot\lambda_p = \left[\frac{\langle f(\boldsymbol{\tau}, \boldsymbol{\alpha}, R)\rangle}{K}\right]^m \ , \qquad \dot\lambda_s = \left[\frac{J_2(\boldsymbol{\alpha})}{a}\right]^r$$

Evolution equations of stress-like internal variables:

$$\mathring{\boldsymbol{\alpha}} = \frac{\partial^2 \Psi}{\partial\, \boldsymbol{\xi}\, \partial\, \boldsymbol{\xi}}\mathring{\boldsymbol{\xi}} = \left[\frac{\boldsymbol{s} - \boldsymbol{\alpha}}{J_2(\boldsymbol{s} - \boldsymbol{\alpha})} - \frac{\gamma(p)\,\boldsymbol{\alpha}}{a}\right] C\dot\lambda_p - \frac{d\,\boldsymbol{\alpha}}{J_2(\boldsymbol{\alpha})}\dot\lambda_s \ ,$$

$$\dot R = \frac{\partial^2 \Psi}{\partial p \partial p}\dot p = b(Q - R)\dot\lambda_p$$

is the plastic logarithmic strain with spatial description. About the equivalence a detailed account in Lin (2002a) can be consulted. It can be easily proven that the trace of $\mathring{\boldsymbol{h}}^{\log} - \mathring{\boldsymbol{h}}^e$ equals $\dot J^p$, with $J^p = \det \boldsymbol{F}^p$, i.e. the trace stands for the volume rate of the plastic deformation. Since $\boldsymbol{s}$ is a deviatoric tensor we know from $(3.12)_1$ that the back stress $\boldsymbol{\alpha}$ must be deviatoric. This characteristic

is consistent with most theories of metal plasticity. Further, we know from $(3.11)_1$ that $\dot{J}^p \equiv 0$. This means that the isochoric plastic deformation can be automatically furnished in the present constitutive law.

For the convenience of the following numerical implementation the complete finite strain constitutive setting is summarized in table 3.1.

4 Algorithm aspects

In this chapter we present the numerical algorithm of determining the stress responses provided by the finite strain viscoplastic law. Since the constitutive law is nonlinear, the global Newton iterative procedure must be applied so that the stress field can be updated step by step. In this procedure the entire loading process must be divided into a sequence of loading steps. Correspondingly, the entire time interval $[0,\, T]$ is segmented into $[0,\, T] = \bigcup_{n=0}^{m} \mathbb{I}_n$, with $\mathbb{I}_n = [t_n,\, t_{n+1}]$ denoting a time interval. We assume that the constitutive state at instant t_n is given. This means that we know the deformation gradient $\boldsymbol{F}_n$, the stress $\boldsymbol{\tau}_n$, as well as all internal variables $\boldsymbol{h}^e_n$, $\boldsymbol{\xi}_n$, p_n, $\boldsymbol{\alpha}_n$ and R_n at this instant. Further, it is assumed that the deformation gradient $\boldsymbol{F}_{n+1}$ at instant t_{n+1} is known, the goal of the numerical algorithm is to determine the internal variables $\boldsymbol{h}^e_{n+1}$, $\boldsymbol{\xi}_{n+1}$, p_{n+1}, $\boldsymbol{\alpha}_{n+1}$, R_{n+1} and the stress $\boldsymbol{\tau}_{n+1}$ at time t_{n+1}.

4.1 Local discrete evolution equations

According to remarks 3.1 and 3.2 (see also equation (3.11)) we know that in the present constitutive setting the corotational rates $\mathring{\boldsymbol{h}}^e$, $\mathring{\boldsymbol{\xi}}$ and $\mathring{\boldsymbol{h}}^{\log}$ are always coaxial. Therefore, the principal axes of the three rate tensors corotate in phase with the logarithmic corotational coordinate frame. In the same way, the corotational rate $\mathring{\boldsymbol{\alpha}}$ is also coaxial to the above three rate tensors. Let $\Delta\boldsymbol{Q}$ be the rotation increment of the coordinate frame over time increment $\Delta t = t_{n+1} - t_n$. Then, the elastic logarithmic strain $\boldsymbol{h}^e_{n+1}$ and the internal variable $\boldsymbol{\alpha}_{n+1}$ at instant t_{n+1} can be expressed by virtue of a backward Euler scheme as

$$\boldsymbol{h}^e_{n+1} = \Delta\boldsymbol{Q}\boldsymbol{h}^e_n\Delta\boldsymbol{Q}^{\mathrm{T}} + \mathring{\boldsymbol{h}}^e_{n+1}\Delta t\ , \qquad \boldsymbol{\alpha}_{n+1} = \Delta\boldsymbol{Q}\boldsymbol{\alpha}_n\Delta\boldsymbol{Q}^{\mathrm{T}} + \mathring{\boldsymbol{\alpha}}_{n+1}\Delta t\ . \tag{4.1}$$

Because of the coaxiality of $\mathring{\boldsymbol{h}}^e$ and $\mathring{\boldsymbol{h}}^{\log}$ we know that $\boldsymbol{h}^{e\,\mathrm{tr}}_{n+1}$ defined by

$$\boldsymbol{h}^{e\,\mathrm{tr}}_{n+1} = \Delta\boldsymbol{Q}\boldsymbol{h}_n\Delta\boldsymbol{Q}^{\mathrm{T}} + \mathring{\boldsymbol{h}}^e_{n+1}\Delta t\ , \tag{4.2}$$

should also be a logarithmic strain. Where $\boldsymbol{h}_n$ stands for the (total) logarithmic strain at time t_n. In what follows $\boldsymbol{h}^{e\,\mathrm{tr}}$ is called trial elastic logarithmic strain. With these tensors in hand application of the backward Euler scheme to equation $(3.11)_{1,3}$ and (3.12) yields the local discrete evolution

equations

$$\begin{aligned}
\boldsymbol{h}^{e}_{n+1} &= \boldsymbol{h}^{e\,\mathrm{tr}}_{n+1} - \frac{3}{2}\frac{\boldsymbol{s}_{n+1}-\boldsymbol{\alpha}_{n+1}}{J_2(\boldsymbol{s}_{n+1}-\boldsymbol{\alpha}_{n+1})}\Delta\lambda_{p\,n+1}\,,\\
\boldsymbol{\alpha}_{n+1} &= \Delta\boldsymbol{Q}\boldsymbol{\alpha}_n\Delta\boldsymbol{Q}^{\mathrm{T}} + \left[\frac{\boldsymbol{s}_{n+1}-\boldsymbol{\alpha}_{n+1}}{J_2(\boldsymbol{s}_{n+1}-\boldsymbol{\alpha}_{n+1})} - \frac{\gamma(p_{n+1})\,\boldsymbol{\alpha}_{n+1}}{a}\right] C\,\Delta\lambda_{p\,n+1} - \frac{d\,\boldsymbol{\alpha}_{n+1}}{J_2(\boldsymbol{\alpha}_{n+1})}\Delta\lambda_{s\,n+1}\,, \qquad (4.3)\\
R_{n+1} &= R_n + b(Q-R_{n+1})\Delta\lambda_{p\,n+1}\,,\\
p_{n+1} &= p_n + \Delta\lambda_{p\,n+1}\,.
\end{aligned}$$

Here, $\Delta\lambda_{p\,n+1} = \dot{\lambda}_{p\,n+1}\Delta t$ and $\Delta\lambda_{s\,n+1} = \dot{\lambda}_{s\,n+1}\Delta t$. This algorithm is similar to the return mapping algorithm for the rate-independent plasticity, although here the stress can stay outside the yield surface. Obviously, these evolution equations are implicit. For solving them a Newton iterative procedure is usually needed. In equation (4.3) the discrete evolution equation for $\boldsymbol{\xi}_{n+1}$ is not applied, as in the constitutive setting all evolution equations are not directly dependent on the strain-like internal variable $\boldsymbol{\xi}$.

Remark 4.1. Obviously, the above formulated discrete evolution equations depend on the rotation tensor $\Delta\boldsymbol{Q}$. For the computation of this rotation tensor, one can apply the logarithmic spin tensor (see Xiao et al. (1998a,b)) specifying the rotation of the logarithmic corotational coordinate frame and make use of a complicated exponential mapping procedure (see e.g. Simo and Hughes (1998), pp. 297). But, we can in fact circumvent this complicated procedure by exploiting the above mentioned coaxiality and developing the numerical algorithm in the principal value space of the involved coaxial tensors.

Remark 4.2. One can compute the trial elastic logarithmic strain $\boldsymbol{h}^{e\,\mathrm{tr}}_{n+1}$ without using the formulation (4.2). Let $\boldsymbol{f} = \boldsymbol{F}_{n+1}\boldsymbol{F}_n^{-1}$ be a local relative deformation gradient, with $\boldsymbol{F}_{n+1}$ and $\boldsymbol{F}_n^{-1}$ denoting the deformation gradients of an material particle at times t_{n+1} and t_n, respectively. Let $\boldsymbol{b}^e_n = \exp(2\boldsymbol{h}^e_n)$ denote the elastic left Cauchy-Green tensor at time t_n. By exploiting the coaxiality of $\overset{\circ}{\boldsymbol{h}}{}^{\log}$ and $\overset{\circ}{\boldsymbol{h}}{}^{e}$ (i.e. the coaxiality of $\boldsymbol{h}$ and $\boldsymbol{h}^e$) we can formulate the trial elastic left Cauchy-Green tensor $\boldsymbol{b}^{e\,\mathrm{tr}}_{n+1}$ and the trial elastic logarithmic strain $\boldsymbol{h}^{e\,\mathrm{tr}}_{n+1}$ at time t_{n+1} as

$$\boldsymbol{b}^{e\,\mathrm{tr}}_{n+1} = \boldsymbol{f}\,\boldsymbol{b}^e_n\,\boldsymbol{f}^{\mathrm{T}}\,, \qquad \boldsymbol{h}^{e\,\mathrm{tr}}_{n+1} = \tfrac{1}{2}\ln\boldsymbol{b}^{e\,\mathrm{tr}}_{n+1}\,. \qquad (4.4)$$

Since the trial elastic logarithmic strain $\boldsymbol{h}^{e\,\mathrm{tr}}_{n+1}$ is known before the plastic return mapping, the following return mapping algorithm will be formulated in the principal space specified by the trial elastic strain.

4.2 Return mapping algorithm in principal stresses

Application of the spectral decomposition to the trial elastic logarithmic strain $\boldsymbol{h}^{e\,\mathrm{tr}}$ yields

$$\boldsymbol{h}^{e\,\mathrm{tr}} = \sum_{A=1}^{3} h^{e\,\mathrm{tr}}_A\,\boldsymbol{n}^{e\,\mathrm{tr}}_A \otimes \boldsymbol{n}^{e\,\mathrm{tr}}_A\,, \qquad (4.5)$$

with $h_A^{e\,\mathrm{tr}}$ being the eigenvalues, $\boldsymbol{n}_A^{e\,\mathrm{tr}}$ the orthonormal eigenvectors of $\boldsymbol{h}^{e\,\mathrm{tr}}$, respectively. As the rank-two tensors $\boldsymbol{h}^e$, $\boldsymbol{\tau}$, $\boldsymbol{s}$ and $\boldsymbol{\alpha}$ are coaxial to $\boldsymbol{h}^{e\,\mathrm{tr}}$, their spectral decomposition can be carried out in the principal space specified by the eigenvectors $\boldsymbol{n}_A^{e\,\mathrm{tr}}$. This means that the evolutions of the principal directions of these tensors are specified by the trial elastic state, only the evolutions of the eigenvalues of these tensors follow the return mapping process. Therefore, we should recast the discrete evolution equations (4.3) in terms of the eigenvalues of the involved tensors. In order to make the following formulations compact, we make use of the vector notations

$$\boldsymbol{\beta} = \begin{bmatrix} \tau_1 \\ \tau_2 \\ \tau_3 \end{bmatrix} , \quad \bar{\boldsymbol{\beta}} = \begin{bmatrix} s_1 \\ s_2 \\ s_3 \end{bmatrix} , \quad \boldsymbol{\eta}^e = \begin{bmatrix} h_1^e \\ h_2^e \\ h_3^e \end{bmatrix} , \quad \boldsymbol{\eta}^{e\,\mathrm{tr}} = \begin{bmatrix} h_1^{e\,\mathrm{tr}} \\ h_2^{e\,\mathrm{tr}} \\ h_3^{e\,\mathrm{tr}} \end{bmatrix} , \quad \boldsymbol{\theta} = \begin{bmatrix} \alpha_1 \\ \alpha_2 \\ \alpha_3 \end{bmatrix} , \tag{4.6}$$

to describe the eigenvalues of the corresponding tensors $\boldsymbol{\tau}, \boldsymbol{s}, \boldsymbol{h}^e, \boldsymbol{h}^{e\,\mathrm{tr}}$ and $\boldsymbol{\alpha}$, respectively. Application of these notations to $(4.3)_{1,2}$, with recalling that the rotation push-forward $\Delta\boldsymbol{Q}\boldsymbol{\alpha}_n\Delta\boldsymbol{Q}^{\mathrm{T}}$ does not change the eigenvalues of $\boldsymbol{\alpha}_n$, yields

$$\begin{aligned} \boldsymbol{\eta}^e_{n+1} &= \boldsymbol{\eta}^{e\,\mathrm{tr}}_{n+1} - \frac{3}{2}\frac{\bar{\boldsymbol{\beta}}_{n+1} - \boldsymbol{\theta}_{n+1}}{J_2(\bar{\boldsymbol{\beta}}_{n+1} - \boldsymbol{\theta}_{n+1})}\Delta\lambda_{p\,n+1} , \\ \boldsymbol{\theta}_{n+1} &= \boldsymbol{\theta}_n + \left[\frac{\bar{\boldsymbol{\beta}}_{n+1} - \boldsymbol{\theta}_{n+1}}{J_2(\bar{\boldsymbol{\beta}}_{n+1} - \boldsymbol{\theta}_{n+1})} - \frac{\gamma(p_{n+1})\,\boldsymbol{\theta}_{n+1}}{a}\right] C\Delta\lambda_{p\,n+1} - \frac{d\,\boldsymbol{\theta}_{n+1}}{J_2(\boldsymbol{\theta}_{n+1})}\Delta\lambda_{s\,n+1} , \end{aligned} \tag{4.7}$$

Equations (4.7) and $(4.3)_{3,4}$ constitute the discrete evolution equations in principal stresses. In these evolution equations the unknowns $\boldsymbol{\eta}^e_{n+1}$, $\bar{\boldsymbol{\beta}}_{n+1}$, $\boldsymbol{\theta}_{n+1}$, $\dot{\lambda}_{p\,n+1}\Delta t$, $\dot{\lambda}_{s\,n+1}\Delta t$, p_{n+1} and R_{n+1} are involved. It is obvious that these unknowns cannot be determined just by these discrete evolution equations. Equations (2.12) (with f defined by (3.8)), (2.13) and (3.7) must be applied to complement the equation system of solving these variables. Due to the implicit characteristic of this equation system the Newton iterative scheme must be exploited. Although one can solve the equation system directly by virtue of the Newton scheme a reformulation of the equation system proves convenient for reducing the computation cost.

Let $\boldsymbol{A}$ be a rank-two counterpart of the rank-four elastic tensor, with $\boldsymbol{A} = \lambda\boldsymbol{i}\otimes\boldsymbol{i} + 2\mu\boldsymbol{1}$. Where $\boldsymbol{i} = [1, 1, 1]^{\mathrm{T}}$. Then, the principal stress vector $\boldsymbol{\beta}$, the trial stress vector $\boldsymbol{\beta}^{\mathrm{tr}}$ and their deviatoric counterparts can be expressed as

$$\boldsymbol{\beta} = \boldsymbol{A}\,\boldsymbol{\eta}^e , \qquad \boldsymbol{\beta}^{\mathrm{tr}} = \boldsymbol{A}\,\boldsymbol{\eta}^{e\,\mathrm{tr}} , \qquad \bar{\boldsymbol{\beta}} = 2\mu\bar{\boldsymbol{\eta}}^e , \qquad \bar{\boldsymbol{\beta}}^{e\,\mathrm{tr}} = 2\mu\bar{\boldsymbol{\eta}}^{e\,\mathrm{tr}} . \tag{4.8}$$

Here, $\bar{\boldsymbol{\eta}}^e$ and $\bar{\boldsymbol{\eta}}^{e\,\mathrm{tr}}$ are the eigenvalues of the deviators of $\boldsymbol{h}^e$ and $\boldsymbol{h}^{e\,\mathrm{tr}}$; i.e.

$$\bar{\boldsymbol{\eta}}^e = \begin{bmatrix} \bar{h}_1^e \\ \bar{h}_2^e \\ \bar{h}_3^e \end{bmatrix} , \quad \bar{\boldsymbol{\eta}}^{e\,\mathrm{tr}} = \begin{bmatrix} \bar{h}_1^{e\,\mathrm{tr}} \\ \bar{h}_2^{e\,\mathrm{tr}} \\ \bar{h}_3^{e\,\mathrm{tr}} \end{bmatrix} , \tag{4.9}$$

with $\bar{h}_A^e = h_A^e - \mathrm{tr}\,\boldsymbol{h}^e/3$ and $\bar{h}_A^{e\,\mathrm{tr}} = h_A^{e\,\mathrm{tr}} - \mathrm{tr}\,\boldsymbol{h}^{e\,\mathrm{tr}}/3$, for $A = 1, 2, 3$. Further, let $\bar{\boldsymbol{\nu}} = (\bar{\boldsymbol{\beta}} - \boldsymbol{\theta})/\|\bar{\boldsymbol{\beta}} - \boldsymbol{\theta}\|$. Then, application of equations $(4.8)_{1,2}$ and the definition of $\bar{\boldsymbol{\nu}}$ to $(4.7)_1$ yields $\boldsymbol{\beta}_{n+1} = \boldsymbol{\beta}^{\mathrm{tr}}_{n+1} -$

$\sqrt{\frac{3}{2}}\Delta\lambda_{p\,n+1}\boldsymbol{A}\bar{\boldsymbol{\nu}}_{n+1}$. Due to $\bar{\boldsymbol{\nu}}\cdot\boldsymbol{i}=0$ we have

$$\boldsymbol{\beta}\cdot\boldsymbol{i}=\boldsymbol{\beta}^{\mathrm{tr}}\cdot\boldsymbol{i}\ ,\qquad \bar{\boldsymbol{\beta}}_{n+1}=\bar{\boldsymbol{\beta}}^{\mathrm{tr}}_{n+1}-\sqrt{6}\mu\Delta\lambda_{p\,n+1}\bar{\boldsymbol{\nu}}_{n+1}\ . \tag{4.10}$$

From $(4.7)_2$ one can derive

$$\boldsymbol{\theta}_{n+1}=\left[\boldsymbol{\theta}_n+\sqrt{\tfrac{2}{3}}\,C\Delta\lambda_{p\,n+1}\bar{\boldsymbol{\nu}}_{n+1}\right]/M_{n+1}\ , \tag{4.11}$$

where $M_{n+1}=1+C\Delta\lambda_{p\,n+1}\gamma(p_{n+1})/a+d\Delta\lambda_{s\,n+1}/J_2(\boldsymbol{\theta}_{n+1})$. It should be noted here that M_{n+1} can be treated as a function of the independent back stress $\boldsymbol{\theta}_{n+1}$ and plastic multiplier $\Delta\lambda_{p\,n+1}$, since the other two variables: the accumulated plastic strain p_{n+1} and the static recovery multiplier $\Delta\lambda_{s\,n+1}$ depend explicitly on $\Delta\lambda_{p\,n+1}$ and $\boldsymbol{\theta}_{n+1}$, respectively. See (2.13) and $(4.3)_4$. Subtraction of (4.11) from $(4.10)_2$ implies

$$\bar{\boldsymbol{\beta}}_{n+1}-\boldsymbol{\theta}_{n+1}=(\bar{\boldsymbol{\beta}}^{\mathrm{tr}}_{n+1}-\boldsymbol{\theta}_n/M_{n+1})-\sqrt{\tfrac{2}{3}}(3\mu+C/M_{n+1})\Delta\lambda_{p\,n+1}\bar{\boldsymbol{\nu}}_{n+1} \tag{4.12}$$

According to the definition of $\bar{\boldsymbol{\nu}}$ we know that $\bar{\boldsymbol{\beta}}_{n+1}-\boldsymbol{\theta}_{n+1}$ is coaxial to $\bar{\boldsymbol{\nu}}_{n+1}$. Therefore, we have

$$\bar{\boldsymbol{\nu}}_{n+1}=(\bar{\boldsymbol{\beta}}^{\mathrm{tr}}_{n+1}-\boldsymbol{\theta}_n/M_{n+1})/\|\bar{\boldsymbol{\beta}}^{\mathrm{tr}}_{n+1}-\boldsymbol{\theta}_n/M_{n+1}\|\ . \tag{4.13}$$

It can be easily seen from this equation that $\bar{\boldsymbol{\nu}}_{n+1}$ is dependent on $\Delta\lambda_{p\,n+1}$ and $\boldsymbol{\theta}_{n+1}$, but independent of the principal stress vector $\boldsymbol{\beta}_{n+1}$. Therefore, equation (4.11) also depends on the two variables $\Delta\lambda_{p\,n+1}$ and $\boldsymbol{\theta}_{n+1}$ only. By making use of (2.12) (with the yield function f defined by (3.8)) and (4.12) we can derive another implicit equation for the plastic loading situations

$$\Delta\lambda_{p\,n+1}=\Delta t\left[\frac{\langle J_2(\bar{\boldsymbol{\beta}}^{\mathrm{tr}}_{n+1}-\boldsymbol{\theta}_n/M_{n+1})-(3\mu+C/M_{n+1})\Delta\lambda_{p\,n+1}-k-R_{n+1}\rangle}{K}\right]^m\ . \tag{4.14}$$

Obviously, this equation also includes two variables $\Delta\lambda_{p\,n+1}$ and $\boldsymbol{\theta}_{n+1}$ only. Therefore, equations (4.11) and (4.14) consist of an implicit equation set, which can be used to solve the back stress $\boldsymbol{\theta}_{n+1}$ and the plastic multiplier $\Delta\lambda_{p\,n+1}$. After getting the two variables the other quantities at time t_{n+1} can be trivially determined by the corresponding explicit equations.

Remark 4.3. If the static recovery effect is omitted (i.e. $\dot{\lambda}_s\equiv 0$) M_{n+1}, and therefore, $\bar{\boldsymbol{\nu}}_{n+1}$ and $\boldsymbol{\theta}_{n+1}$ can be expressed as the explicit functions of the plastic multiplier $\Delta\lambda_{p\,n+1}$. In this situation equation (4.14) is independent of the back stress $\boldsymbol{\theta}_{n+1}$. The only needed local iterative procedure is for solving $\Delta\lambda_{p\,n+1}$ from equation (4.14). Further, if the relaxation effect is also negligible (i.e. $\gamma(p)\equiv 0$) the constitutive model reduces to the classical unified viscoplastic model of J_2-flow theory. In this case $M_{n+1}=1$, and $\bar{\boldsymbol{\nu}}_{n+1}=(\bar{\boldsymbol{\beta}}^{\mathrm{tr}}_{n+1}-\boldsymbol{\theta}_n)/\|\bar{\boldsymbol{\beta}}^{\mathrm{tr}}_{n+1}-\boldsymbol{\theta}_n\|$ is constant in the return mapping process.

4.3 Consistent elastoplastic tangent moduli

In finite element implementation of a mechanical field problem the central field equation necessarily to be solved is the spatial discrete equation derived from the weak form of the balance equation

of linear momentum. By linearization of the weak form of the balance equation one can obtain the definition of the exact consistent or algorithmic tangent moduli. With spatial description and omitting the subscript $n+1$ the definition of the consistent tangent moduli is included in the rate equation

$$\pounds_v \boldsymbol{\tau} = \mathbb{C}^{ep} : \boldsymbol{d} \,. \tag{4.15}$$

Where $\mathbb{C}^{ep}$ is the consistent tangent moduli, while $\pounds_v \boldsymbol{\tau}$ and $\boldsymbol{d}$ denote the Lie-derivative of the Kirchhoff stress $\boldsymbol{\tau}$ with respect to the "flow" specified by the total deformation and the deformation rate tensor, respectively. About the detailed formulation of (4.15) we refer to Simo (1998), pp. 365–368. Equation (4.15) is equivalent to

$$\dot{\boldsymbol{S}} = \boldsymbol{\varphi}^*(\mathbb{C}^{ep}) : \dot{\boldsymbol{C}}/2 \,, \tag{4.16}$$

with $\boldsymbol{\varphi}^*(\bullet)$ being the pull-back of the argument $(\bullet)$ by the map $\boldsymbol{\varphi}$, which defines the current configuration. $\boldsymbol{S}$ and $\boldsymbol{C}$ denote the second Piola-Kirchhoff stress tensor and the right Cauchy-Green deformation tensor, respectively. According to the multiplicative decomposition of (3.1) the pull-back $\boldsymbol{\varphi}(\bullet)$ is equivalent to $\boldsymbol{\varphi}^{p*}(\boldsymbol{\varphi}^{e*}(\bullet))$, with $\boldsymbol{\varphi}^{e*}(\bullet)$ and $\boldsymbol{\varphi}^{p*}(\bullet)$ being the pull-back operations associated respectively with the local deformation gradients $\boldsymbol{F}^e$ and $\boldsymbol{F}^p$. Since the plastic state is "frozen" in the return mapping process the composition map $\boldsymbol{\varphi}^e = \boldsymbol{\varphi} \circ \boldsymbol{\varphi}^{p-1}$ is in fact a trial elastic map. Let $\boldsymbol{T}$ and $\boldsymbol{C}^e$ be respectively the second Piola-Kirchhoff stress tensor and the trial elastic right Cauchy-Green tensor in the intermediate configuration. Then, we have $\dot{\boldsymbol{S}} = \boldsymbol{F}^{p-1}\dot{\boldsymbol{T}}\boldsymbol{F}^{p-\mathrm{T}}$, $\dot{\boldsymbol{C}} = \boldsymbol{F}^{p\mathrm{T}}\dot{\boldsymbol{C}}^e\boldsymbol{F}^p$ and

$$\dot{\boldsymbol{T}} = \boldsymbol{\varphi}^p_*(\boldsymbol{\varphi}^*(\mathbb{C}^{ep})) : \dot{\boldsymbol{C}}^e/2 = \boldsymbol{\varphi}^{e*}(\mathbb{C}^{ep}) : \dot{\boldsymbol{C}}^e/2 \,. \tag{4.17}$$

Where $\boldsymbol{\varphi}^p_*(\bullet)$ denotes the push-forward of the argument $(\bullet)$ by the map $\boldsymbol{\varphi}^p$ in connection with the plastic deformation gradient $\boldsymbol{F}^p$. Here, it should be noted that for the present viscoplastic law (a strain-driven law) the algorithmic return mapping process is driven by the trial elastic deformation. Therefore, in the return mapping process the second Piola-Kirchhoff stress $\boldsymbol{T}$, as the pull-back of the spatial Kirchhoff stress $\boldsymbol{\tau}$ by the trial elastic map $\boldsymbol{\varphi}^e$, should be a functional of the trial elastic deformation $\boldsymbol{C}^e$. Then, we have the relation $\dot{\boldsymbol{T}} = (\partial \boldsymbol{T}/\partial \boldsymbol{C}^e) : \dot{\boldsymbol{C}}^e$. Comparison of this relation with equation (4.17) yields

$$\boldsymbol{\varphi}^{e*}(\mathbb{C}^{ep}) = 2\partial \boldsymbol{T}/\partial \boldsymbol{C}^e \quad \Longleftrightarrow \quad \mathbb{C}^{ep} = 2\,\boldsymbol{\varphi}^e_*\,(\partial \boldsymbol{T}/\partial \boldsymbol{C}^e) \,. \tag{4.18}$$

Here, $\boldsymbol{\varphi}^e_*(\bullet)$ denotes the push-forward of the argument $(\bullet)$ by the map $\boldsymbol{\varphi}^e$ associated with the trial elastic deformation gradient. In our constitutive setting the Kirchhoff stress $\boldsymbol{\tau}$, the elastic logarithmic strain $\boldsymbol{h}^e$ and the trial elastic logarithmic strain $\boldsymbol{h}^{e\,\mathrm{tr}}$ are coaxial. Therefore, $\boldsymbol{C}^e$ and $\boldsymbol{T}$ have identical principal axes. By using the spectral decompositions of $\boldsymbol{C}^e$ and $\boldsymbol{T}$ one can derive

their material time derives

$$\dot{\boldsymbol{C}}^e = \sum_{A=1}^{3} 2\lambda_A^{e\,\mathrm{tr}}\,\dot{\lambda}_A^{e\,\mathrm{tr}}\boldsymbol{N}_A^{e\,\mathrm{tr}}\otimes\boldsymbol{N}_A^{e\,\mathrm{tr}} + \sum_{A,B=1,A\neq B}^{3}\Omega_{AB}\left[(\lambda_B^{e\,\mathrm{tr}})^2-(\lambda_A^{e\,\mathrm{tr}})^2\right]\boldsymbol{N}_A^{e\,\mathrm{tr}}\otimes\boldsymbol{N}_B^{e\,\mathrm{tr}}\,,$$
$$\dot{\boldsymbol{T}} = \sum_{A,B=1}^{3}\frac{\partial T_A}{\partial\lambda_B^{e\,\mathrm{tr}}}\dot{\lambda}_B^{e\,\mathrm{tr}}\boldsymbol{N}_A^{e\,\mathrm{tr}}\otimes\boldsymbol{N}_A^{e\,\mathrm{tr}} + \sum_{A,B=1,A\neq B}^{3}\Omega_{AB}\left[(\lambda_B^{e\,\mathrm{tr}})^2-(\lambda_A^{e\,\mathrm{tr}})^2\right]\frac{T_B-T_A}{(\lambda_B^{e\,\mathrm{tr}})^2-(\lambda_A^{e\,\mathrm{tr}})^2}\boldsymbol{N}_A^{e\,\mathrm{tr}}\otimes\boldsymbol{N}_B^{e\,\mathrm{tr}}\,. \tag{4.19}$$

Here, $\lambda_A^{e\,\mathrm{tr}} = \exp h_A^{e\,\mathrm{tr}}$ are the eigenvalues of the trial elastic right stretch tensor $\sqrt{\boldsymbol{C}^e}$, while $\boldsymbol{N}_A^{e\,\mathrm{tr}}$, with $\|\boldsymbol{N}_A^{e\,\mathrm{tr}}\| = 1$, denote the eigenvectors of $\boldsymbol{C}^e$. Ω_{AB} stands for the components of the spin tensor describing the rotation of the principal vectors $\boldsymbol{N}^{e\,\mathrm{tr}}$. The eigenvalues T_A of the stress $\boldsymbol{T}$ are related to the eigenvalues τ_A of the Kirchhoff stress $\boldsymbol{\tau}$ by $T_A = \tau_A/(\lambda_A^{e\,\mathrm{tr}})^2$. Let $\bar{\mathbb{C}}^{ep} = 2\partial\boldsymbol{T}/\partial\boldsymbol{C}^e$. Then, comparing $(4.19)_2$ with $(4.19)_1$ we arrive at

$$\begin{aligned}\bar{\mathbb{C}}^{ep} = &\sum_{A,B=1}^{3}\frac{1}{\lambda_B^{e\,\mathrm{tr}}}\frac{\partial T_A}{\partial\lambda_B^{e\,\mathrm{tr}}}\boldsymbol{N}_A^{e\,\mathrm{tr}}\otimes\boldsymbol{N}_A^{e\,\mathrm{tr}}\otimes\boldsymbol{N}_B^{e\,\mathrm{tr}}\otimes\boldsymbol{N}_B^{e\,\mathrm{tr}}\\ &+\sum_{A,B=1,A\neq B}^{3}\frac{T_B-T_A}{(\lambda_B^{e\,\mathrm{tr}})^2-(\lambda_A^{e\,\mathrm{tr}})^2}\boldsymbol{N}_A^{e\,\mathrm{tr}}\otimes\boldsymbol{N}_B^{e\,\mathrm{tr}}\otimes(\boldsymbol{N}_A^{e\,\mathrm{tr}}\otimes\boldsymbol{N}_B^{e\,\mathrm{tr}}+\boldsymbol{N}_B^{e\,\mathrm{tr}}\otimes\boldsymbol{N}_A^{e\,\mathrm{tr}})\,.\end{aligned} \tag{4.20}$$

Taking the push-forward operation to (4.20) we can derive

$$\begin{aligned}\mathbb{C}^{ep} = &\sum_{A,B=1}^{3}(c_{AB}^{ep}-2\tau_A\delta_{AB})\boldsymbol{n}_A^{e\,\mathrm{tr}}\otimes\boldsymbol{n}_A^{e\,\mathrm{tr}}\otimes\boldsymbol{n}_B^{e\,\mathrm{tr}}\otimes\boldsymbol{n}_B^{e\,\mathrm{tr}}\\ &+\sum_{A,B=1,A\neq B}^{3}\frac{\tau_A(\lambda_B^{e\,\mathrm{tr}})^2-\tau_B(\lambda_A^{e\,\mathrm{tr}})^2}{(\lambda_A^{e\,\mathrm{tr}})^2-(\lambda_B^{e\,\mathrm{tr}})^2}\boldsymbol{n}_A^{e\,\mathrm{tr}}\otimes\boldsymbol{n}_B^{e\,\mathrm{tr}}\otimes(\boldsymbol{n}_A^{e\,\mathrm{tr}}\otimes\boldsymbol{n}_B^{e\,\mathrm{tr}}+\boldsymbol{n}_B^{e\,\mathrm{tr}}\otimes\boldsymbol{n}_A^{e\,\mathrm{tr}})\,,\end{aligned} \tag{4.21}$$

with

$$c_{AB}^{ep} = \partial\tau_A/\partial h_B^{e\,\mathrm{tr}}\,. \tag{4.22}$$

Here, it should be noted that the formulation of the algorithmic moduli c_{AB}^{ep} is an arduous task, since the stress components τ_A are not directly dependent on the trial elastic strain components $h_B^{e\,\mathrm{tr}}$. For this formulation the stress-strain relation $(4.8)_1$ and almost all evolution equations must be applied. In what follows we use the matrix notation $\boldsymbol{c} = [c_{AB}^{ep}]$. By application of the chain rule, the stress-strain relation $(4.8)_1$ and the evolution equations (4.7) and $(4.3)_{3,4}$ and after a lengthy calculation we get

$$\boldsymbol{c} = \frac{\partial\boldsymbol{\beta}}{\partial\,\boldsymbol{\eta}^{e\,\mathrm{tr}}} = \frac{\partial\boldsymbol{\beta}}{\partial\,\boldsymbol{\eta}^{e}}\frac{\partial\,\boldsymbol{\eta}^{e}}{\partial\,\boldsymbol{\eta}^{e\,\mathrm{tr}}} = \boldsymbol{A}\boldsymbol{k}^{-1}\,, \tag{4.23}$$

with $\boldsymbol{A}$ being the rank-two elastic moduli used in (4.8), $\boldsymbol{k}$ denoting a rank-two tensor. About the detailed formulation of $\boldsymbol{k}$ see Appendix A.

5 Numerical examples

In oder to prove the effectivity of the extended material law and the numerical algorithm several numerical examples are presented in this chapter. In the first example the consistency of the equation describing the stress evolution with elasticity is numerically proven. In the second example a comparison between a numerical prediction of the extended law and an experimental observation is carried out and a good agreement can be found. Example three shows the constitutive behavior of the finite viscoplastic law at simple shear with finite rotation. Finally, the mechanical responses described by this material law in upsetting of an axisymmetric billet is presented.

5.1 Elastic stress response of a closed deformation process

Since the recent two decades it has been found that the elasticity-inconsistent equations describing stress evolution in an inelastic constitutive law usually cause unrealistic stress responses at specific deformation processes with finite rotation. A well-known example is the unrealistic oscillatory stress response provided by the plasticity theories using the Jaumann formulations at simple shear and under kinematic hardening. This oscillatory stress response attributes to the Jaumann formulation of the stress evolution equation. Theoretically, it can been found that the stress equation in the present law is formulated hyperelastically. Therefore, it is consistent with elasticity. In this example we still prove the consistency numerically by observing the stress response presented by this law in an elastic deformation process. By selecting a large yield stress we enforce the viscoplastic law to describe purely elastic behavior. Now, we consider the closed deformation process shown in

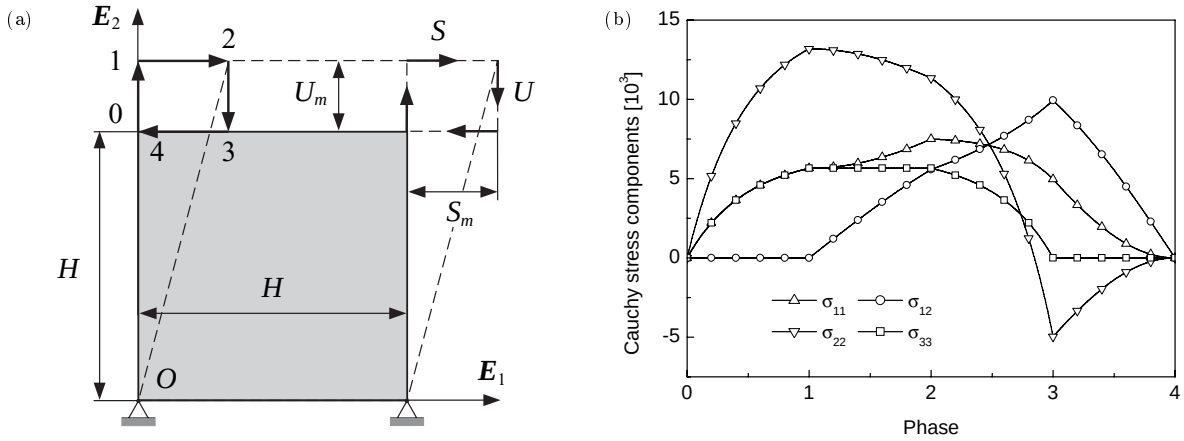

Figure 5.1: (a) Closed deformation path with four phases, (b) Cauchy stress vs deformation phases.

Fig. 5.1(a). The material element with initial square section is subject to four deformation phases: tension (0–1), shear (1–2), compression (2–3) and inverse shear (3–4). It is assumed that there is no strain in the third direction. Thus, the material element always keeps in state of plane strain. The maxima of the vertical and horizontal displacements U_m and S_m are selected as $U_m/H = 0.8$ and $S_m/H = 1.0$ for the present numerical simulation. The used material constants are Young's modulus $E = 30000$ and Poisson's ratio $\nu = 0.3$. The stress response under the given deformation geometry and material condition is shown in Fig. 5.1(b). It can be easily seen that at the end of the closed deformation process all stress components go back to zero. This characteristic is obviously consistent with elastic behavior. In addition, we note that the current formulation of stress evolution equation can present unique stress response at an elastic deformation state in spite of the difference of paths for reaching that state. Therefore, the corresponding formulation is elasticity-consistent.

5.2 Comparison with experimental observation at cyclic uniaxial loading

In this example a comparison of a prediction of the viscoplastic law with experimental results at cyclic uniaxial loading is carried out. Limited by the existing experimental data this comparison is accomplished only at infinitesimal deformations. Fig. 5.2(a) shows the history of the strain component ε_{22} in a cyclic uniaxial loading process. ε_{22} denotes the normal strain component lying in the loading direction. Under total 23 cycles the first 22 cycles have an identical strain trace. In the last strain cycle the strain keeps constant at maximum and minimum respectively in the time intervals [910, 940] s and [960, 990] s. Fig. 5.2(b) illustrates the experimental observation and the numerical simulation in the last strain cycle. The experimental data are obtained from a cyclic uniaxial test on a cylinder made of the Ni-based super alloy IN 738 LC at 850 °C (Olschewski et al., 1991). The material constants used for the numerical prediction are $\lambda = 109209.42$ MPa, $\mu = 56259.40$ MPa, $k = 153$ MPa, $C = 62511$ MPa, $b = 317$, $Q = -153$ MPa, $K = 1150$ MPa·s$^{1/m}$, $m = 7.7$, $a = 311$ MPa, $r = 4.8$, $d = 0.0227$ MPa/s, $\gamma_\infty = 1.1$ and $\omega = 0.04$. From

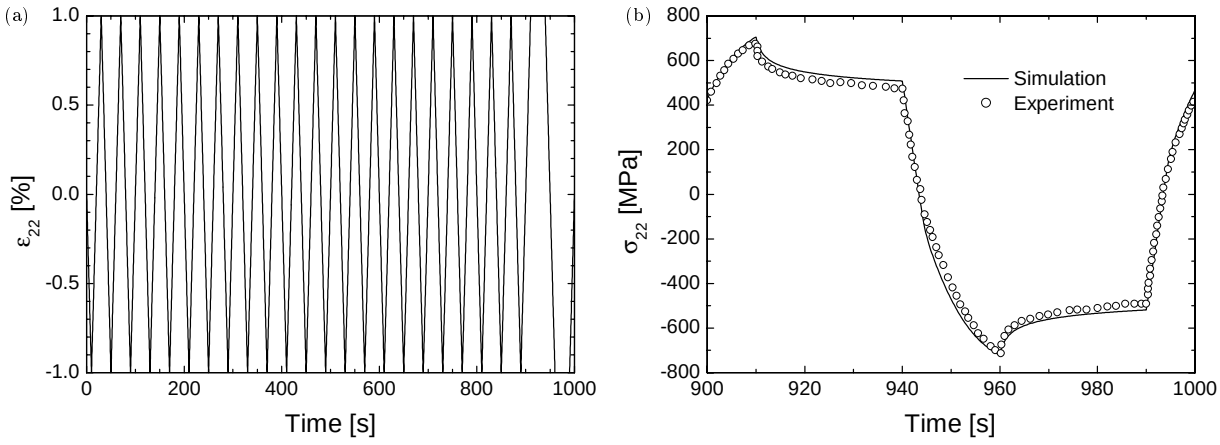

Figure 5.2: Cyclic uniaxial tension and compression. (a) Strain history, (b) stress vs time, the last cycle.

Fig. 5.2(b) it can be seen that after 22 strain cycles the numerical prediction provided by this theory agrees still very well with the experimental observation. This proves that the extended viscoplastic law is effective even at complex cyclic loading.

5.3 Stress response at simple shear

The reason for investigating the stress response presented by the extended material law at simple shear comes from the facts that at simple shear large rotation can be easily accomplished and some rate-independent and rate-dependent plasticity laws render unrealistic stress responses. For this numerical example we also apply the material constants of the Ni-based super alloy IN 738 LC at 850 °C given in the last subsection. The used engineering shear strain rate is $\dot{\gamma}_{12} = 0.007\ \mathrm{s}^{-1}$. All nonzero stress components σ_{11}, σ_{22} and σ_{12} are illustrated in Fig. 5.3(a) and (b). Obviously, after reaching the plastic state all three stress components keep almost constant values with the increasing shear strain γ_{12}. For the first two stress components there is the relation $\sigma_{22} = -\sigma_{11}$. Here, there is no the unrealistic oscillatory stress response presented by some plasticity theories at simple shear.

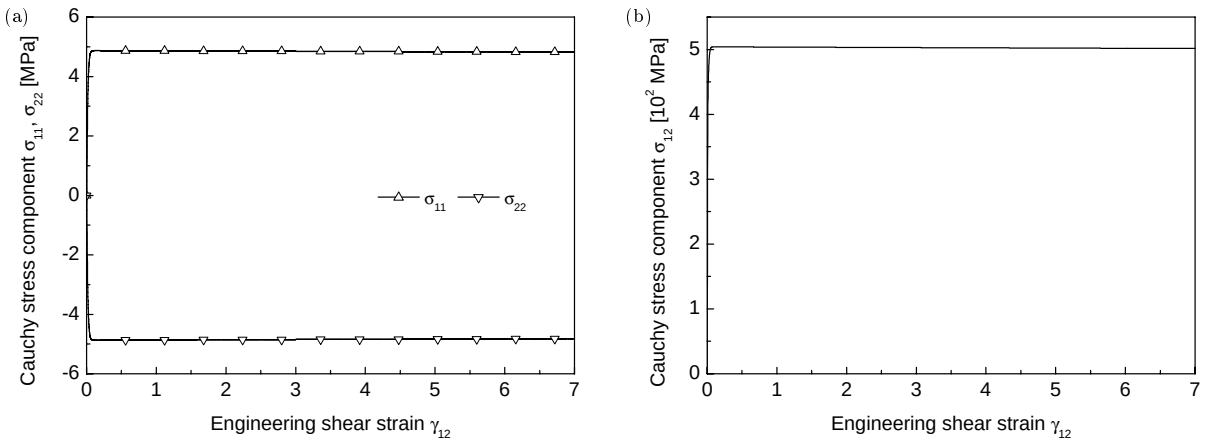

Figure 5.3: Cauchy stress response at simple shear, $\dot{\gamma}_{12} = 0.007\ \mathrm{s}^{-1}$. (a) σ_{11} and σ_{22}, (b) σ_{12}

5.4 Mechanical response of an axisymmetric billet in upsetting

In this subsection the upsetting of an axisymmetric billet is numerically simulated. Here, we assume that the material of the billet is again the Ni-based super alloy IN738 LC and we apply the above recorded material constants in this simulation. In the original state the billet has a radius of 10 mm and a height of 30 mm. In ten seconds it is uniformly upset to 38% original height. Then, this upsetting is kept for one second. In Fig. 5.4(a) the history of the axial reaction force is illustrated. It can be seen that at the beginning the reaction force increases rapidly. In this phase the global deformation is elastic. Then, the billet goes into a global plastic state and the reaction force increases slowly. After 5 s there are five skip points on the curve. These skips are caused by the change of

contact nodes. In the phase of relaxation the curve is smooth and about one third of the reaction force at time 10 s is relaxed. Fig. 5.4(b) shows the initial finite element mesh of one quarter of the billet and the deformed one with isocontours of von Mises stress at time 10 s. This example proves the effectivities of the mathematical model and numerical implementation under severe boundary conditions and deformations.

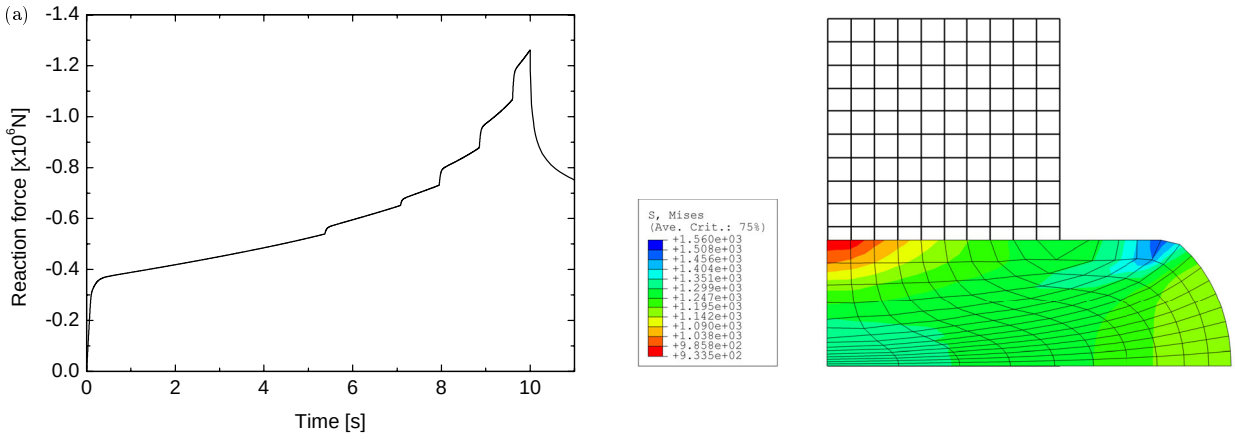

Figure 5.4: Upset of axisymmetric billet. (a) Reaction force vs time, (b) initial finite element mesh and deformed mesh with von Mises stress contours at time 10 s.

6 Conclusions

Limited by their mathematical forms the Chaboche viscoplastic laws can be applied only at infinitesimal deformations. In this work a representative Chaboche viscoplastic law is mathematically extended to the finite strain context based on a new internal dissipation inequality. Therefore, this extension is consistent with the second law of thermodynamics. The extended law is numerically implemented by coding it in a finite element program. Several numerical examples prove that the extended viscoplastic law and the numerical implementation are very effective.

Appendix A

In this appendix the detailed algorithmic moduli tensor $\boldsymbol{k}$ is formulated. For clarity the subscripts $n+1$ of all corresponding quantities are omitted. Here, we record, according to (4.7) and $(4.3)_{3,4}$, a set of discrete evolution equations

$$\begin{aligned}
\boldsymbol{\eta}^{e\,\mathrm{tr}} &= \boldsymbol{\eta}^{e} + \frac{3}{2}\frac{\bar{\boldsymbol{\beta}} - \boldsymbol{\theta}}{J_2(\bar{\boldsymbol{\beta}} - \boldsymbol{\theta})}\Delta\lambda_p \,, \\
\boldsymbol{\theta} &= \boldsymbol{\theta}_n + \left[\frac{\bar{\boldsymbol{\beta}} - \boldsymbol{\theta}}{J_2(\bar{\boldsymbol{\beta}} - \boldsymbol{\theta})} - \frac{\gamma(p)\,\boldsymbol{\theta}}{a}\right] C\Delta\lambda_p - \frac{d\,\boldsymbol{\theta}}{J_2(\boldsymbol{\theta})}\Delta\lambda_s \,, \\
R &= R_n + b(Q - R)\Delta\lambda_p \,, \\
p &= p_n + \Delta\lambda_p \,,
\end{aligned} \tag{A1}$$

with

$$\Delta\lambda_p = \left[\frac{\left\langle J_2(\bar{\boldsymbol{\beta}} - \boldsymbol{\theta}) - k - R\right\rangle}{K}\right]^m \Delta t \,, \qquad \Delta\lambda_s = \left[\frac{J_2(\boldsymbol{\theta})}{a}\right]^r \Delta t \,. \tag{A2}$$

From $(A1)_{3,4}$ we can easily derive

$$\frac{\partial p}{\partial\,\boldsymbol{\eta}^e} = \frac{\partial\Delta\lambda_p}{\partial\,\boldsymbol{\eta}^e} \,, \qquad \frac{\partial R}{\partial\,\boldsymbol{\eta}^e} = A_1\frac{\partial\Delta\lambda_p}{\partial\,\boldsymbol{\eta}^e} \,, \tag{A3}$$

with $A_1 = \frac{b(Q-R_n)}{(1+b\Delta\lambda_p)^2}$. By using the relation $\bar{\boldsymbol{\beta}} = 2\mu\bar{\boldsymbol{\eta}}^e = 2\mu\,\boldsymbol{P}\boldsymbol{\eta}^e$, with $\boldsymbol{P} = \mathbf{1} - \frac{1}{3}\boldsymbol{i}\otimes\boldsymbol{i}$, and the chain rule we arrive at

$$\frac{\partial\bar{\boldsymbol{\beta}}}{\partial\,\boldsymbol{\eta}^e} = 2\mu\,\boldsymbol{P} \,, \qquad \frac{\partial J_2(\bar{\boldsymbol{\beta}} - \boldsymbol{\theta})}{\partial\,\boldsymbol{\eta}^e} = \sqrt{\tfrac{3}{2}}\bar{\boldsymbol{\nu}}\left[2\mu\,\boldsymbol{P} - \frac{\partial\,\boldsymbol{\theta}}{\partial\,\boldsymbol{\eta}^e}\right] \,, \tag{A4}$$

where $\bar{\boldsymbol{\nu}} = (\bar{\boldsymbol{\beta}} - \boldsymbol{\theta})/\|\bar{\boldsymbol{\beta}} - \boldsymbol{\theta}\|$. With the relations $(A3)_2$ and $(A4)_2$ in hand one gets from $(A2)_1$

$$\frac{\partial\Delta\lambda_p}{\partial\,\boldsymbol{\eta}^e} = \sqrt{\tfrac{3}{2}}A_3\bar{\boldsymbol{\nu}}\left[2\mu\,\boldsymbol{P} - \frac{\partial\,\boldsymbol{\theta}}{\partial\,\boldsymbol{\eta}^e}\right] \,, \tag{A5}$$

where $A_3 = \frac{A_2}{1+A_1A_2}$, with $A_2 = \frac{m\Delta t}{K}\left[\frac{\langle J_2(\bar{\boldsymbol{\beta}}-\boldsymbol{\theta})-k-R\rangle}{K}\right]^{m-1}$. Recalling $\gamma(p) = \gamma_\infty + (1-\gamma_\infty)\exp(-\omega p)$, and exploiting equations $(A3)_1$, (A5) we obtain

$$\frac{\partial\gamma(p)}{\partial\,\boldsymbol{\eta}^e} = -\sqrt{\tfrac{3}{2}}A_3\omega(1-\gamma_\infty)\exp(-\omega p)\bar{\boldsymbol{\nu}}\left[2\mu\,\boldsymbol{P} - \frac{\partial\,\boldsymbol{\theta}}{\partial\,\boldsymbol{\eta}^e}\right] \,. \tag{A6}$$

Taking the partial derivative with respect to $\boldsymbol{\eta}^e$ to $(A2)_2$ gives

$$\frac{\partial\Delta\lambda_s}{\partial\,\boldsymbol{\eta}^e} = \sqrt{\tfrac{3}{2}}r\,\Delta\lambda_s/J_2(\boldsymbol{\theta})\bar{\boldsymbol{\nu}}_{\boldsymbol{\theta}}\frac{\partial\,\boldsymbol{\theta}}{\partial\,\boldsymbol{\eta}^e} \,, \tag{A7}$$

with $\bar{\boldsymbol{\nu}}_{\boldsymbol{\theta}} = \boldsymbol{\theta} \,/\, \| \boldsymbol{\theta} \|$.

By taking the partial derivative with respect to $\boldsymbol{\eta}^e$ to equation $(\mathrm{A1})_2$, together with application of the above relations to the corresponding partial derivatives, and after lengthy calculations we come to

$$\frac{\partial \boldsymbol{\theta}}{\partial \boldsymbol{\eta}^e} = \boldsymbol{B}^{-1}\boldsymbol{G} \,, \tag{A8}$$

with

$$\begin{aligned}
\boldsymbol{B} &= B_1\mathbf{1} + B_2\bar{\boldsymbol{\nu}} \otimes \bar{\boldsymbol{\nu}} + B_3\bar{\boldsymbol{\nu}}_{\boldsymbol{\theta}} \otimes \bar{\boldsymbol{\nu}} + B_4\bar{\boldsymbol{\nu}}_{\boldsymbol{\theta}} \otimes \bar{\boldsymbol{\nu}}_{\boldsymbol{\theta}} \,, \\
B_1 &= 1 + C\Delta\lambda_p \left[J_2^{-1}(\bar{\boldsymbol{\beta}} - \boldsymbol{\theta}) + \gamma(p)/a \right] + d\Delta\lambda_s J_2^{-1}(\boldsymbol{\theta}) \,, \\
B_2 &= C\left[A_3 - \Delta\lambda_p J_2^{-1}(\bar{\boldsymbol{\beta}} - \boldsymbol{\theta}) \right] \,, \\
B_3 &= CA_3 J_2(\boldsymbol{\theta})/a \left[(\Delta\lambda_p\omega - 1)\gamma(p) - \omega\gamma_\infty\Delta\lambda_p \right] \,, \\
B_4 &= d\Delta\lambda_s J_2^{-1}(\boldsymbol{\theta})(r-1) \,,
\end{aligned} \tag{A9}$$

and

$$\begin{aligned}
\boldsymbol{G} &= G_1\boldsymbol{P} + G_2\bar{\boldsymbol{\nu}} \otimes \bar{\boldsymbol{\nu}} + G_3\bar{\boldsymbol{\nu}}_{\boldsymbol{\theta}} \otimes \bar{\boldsymbol{\nu}} \,, \\
G_1 &= 2\mu C\Delta\lambda_p J_2^{-1}(\bar{\boldsymbol{\beta}} - \boldsymbol{\theta}) \,, \\
G_2 &= 2\mu C\left[A_3 - \Delta\lambda_p J_2^{-1}(\bar{\boldsymbol{\beta}} - \boldsymbol{\theta}) \right] = 2\mu B_2 \,, \\
G_3 &= 2\mu CA_3 J_2(\boldsymbol{\theta})/a \left[(\Delta\lambda_p\omega - 1)\gamma(p) - \omega\gamma_\infty\Delta\lambda_p \right] = 2\mu B_3 \,.
\end{aligned} \tag{A10}$$

It can be easily seen that all the rank-two tensors $\boldsymbol{B}$, $\boldsymbol{G}$ and $\partial\,\boldsymbol{\theta} \,/\, \boldsymbol{\eta}^e$ are unsymmetric. The unsymmetry comes from the recovery and relaxation behavior included in the model. Taking the partial derivative with respect to $\boldsymbol{\eta}^e$ to equation $(\mathrm{A1})_1$ and exploiting the above related relations we obtain

$$\boldsymbol{k} = \frac{\partial\,\boldsymbol{\eta}^{e\,\mathrm{tr}}}{\partial\,\boldsymbol{\eta}^e} = \mathbf{1} + \tfrac{3}{2}\left[\Delta\lambda_p J_2^{-1}(\bar{\boldsymbol{\beta}} - \boldsymbol{\theta})(\mathbf{1} - \bar{\boldsymbol{\nu}} \otimes \bar{\boldsymbol{\nu}}) + A_3\bar{\boldsymbol{\nu}} \otimes \bar{\boldsymbol{\nu}} \right] \cdot \left[2\mu\boldsymbol{P} - \boldsymbol{B}^{-1}\boldsymbol{G} \right] \,. \tag{A11}$$

Then,

$$\boldsymbol{c} = [c_{AB}^{ep}] = \frac{\partial\boldsymbol{\beta}}{\partial\,\boldsymbol{\eta}^{e\,\mathrm{tr}}} = \frac{\partial\boldsymbol{\beta}}{\partial\,\boldsymbol{\eta}^e}\frac{\partial\,\boldsymbol{\eta}^e}{\partial\,\boldsymbol{\eta}^{e\,\mathrm{tr}}} = \boldsymbol{A}\boldsymbol{k}^{-1} \,. \tag{A12}$$

Obviously, the algorithmic moduli tensor $\boldsymbol{c}$ is also unsymmetric.

References

ABAQUS Theory Manual 5.8 (Hibbitt, Karlsson & Sorensen, Inc., 1998).

Arzt, M., W. Brocks, R. Mohr and W. Qi, User material routine for simulating anisothermal elasto-viscoplasticity and damage, Techincal Note GKSS/WMG/99/11.

Asaro, R.J., Geometrical effects in the inhomogeneous deformation of ductile single crystals, Acta Metallurgica 27 (1979) 445–453.

Asaro, R.J., Micromechanics of crystals and polycrystals, in: Advances in Applied Mechanics, Vol. 23 (Academic Press, New York, 1983).

Asaro, R.J. and J.R. Rice, Strain localization in ductile single crystals, J. Mech. Phy. Solids 25 (1977) 309–338.

Chaboche, J.L., Viscoplastic constitutive equations for the description of cyclic and anisotropic behaviour of metals, Bull. de l'Acad. Polonaise des Sciences, Série Sc. et Tech., 17th Polish Conf. Mech. Solids, Szczyrk, 1975, Vol. 25, pp.33–41.

Chaboche, J.L., Constitutive equations for cyclic plasticity and cyclic viscoplasticity, Int. J. Plasticity. 5 (1989) 247–302.

Chaboche, J.L., Cyclic viscoplastic constitutive equations, part I: A thermodynamically consistent formulation, ASME J. Appl. Mech. 60 (1993) 813–821.

Chaboche, J.L., Cyclic viscoplastic constitutive equations, part II: stored energy—comparison between models and experiments, ASME J. Appl. Mech. 60 (1993) 822–828.

Chaboche, J.L., Thermodynamic formulation of constitutive equations and application to the viscoplasticity and viscoelasticity of metals and polymers, Int. J. Solids Struct. 34 (1997) 2239–2254.

Chaboche, J.L. and O. Jung, Application of a kinematic hardening viscoplasticity model with thresholds to the residual stress relaxation, Int. J. Plasticity 13 (1998) 785–807.

Chaboche, J.L. and G. Rousselier, On the plastic and viscoplastic constitutive equations—Part I: Rules developed with internal variable concept, ASME J. Pressure Vessel Tech. 34 (1983) 153–158.

Chaboche, J.L. and G. Rousselier, On the plastic and viscoplastic constitutive equations—Part II: application of internal variable concepts to the 316 stainless steel, ASME J. Pressure Vessel Tech. 34 (1983) 159–164.

Lemaitre, J. and J.L. Chaboche, Mechanics of Solids Materials (Cambridge University Press, 1990).

Lin, R.C., Viscoelastic and elastic-viscoelastic-elastoplastic constitutive characterizations of polymers at finite strains: theoretical and numerical aspects, PhD Thesis (2002), University of the Federal Armed Forces Hamburg, Germany

Lin, R.C., Numerical study of consistency of rate constitutive equations with elasticity at finite

deformation, Int. J. Num. Methods Engrg. 55 (2002) 1053–1077.

Lin, R.C., Analytical stress solutions of a closed deformation path with stretching and shearing using the hypoelastic formulations, Euro. J. Mech.–A/Solids 22 (2003) 443–461.

Lion, A., A physically based method to represent the thermo-mechanical behaviour of elastomers, Acta Mechanica 123 (1997a) 1–25.

Miehe, C., A constitutive frame of elastoplasticity at large strains based on the notation of a plastic metric, Int. J. Solids Struct. 35 (1998) 3859–3897.

Olschewski, J., R. Sievert and A. Bertram, A comparison of the predictive capabilities of two unified constitutive models at elevated temperatures, in: C.S. Desai et al. eds., Constitutive laws for engineering materials, Proceedings of the Third International Conference on Constitutive Laws for Engineering Materials: Theory and Applications, 1991, New York.

Simo, J.C., Algorithms for static and dynamic multiplicative plasticity that preserve the classical return mapping schemes of the infinitesimal theory, Comput. Methods Appl. Mech. Engrg. 99 (1992) 61–112.

Simo, J.C., Numerical analysis and simulation of plasticity, in: Handbook of Numerical Analyis Vol. IV, P.G. Ciarlet and J.L. Lions eds., Elsevier Science, Amsterdam, 1998.

Simo, J.C. and T.J.R. Hughes, Computational Inelasticity (Springer-Verlag New York Inc., 1998).

Simo, J.C. and C. Miehe, Associative coupled thermoplasticity at finite strains: formulation, numerical Analysis and implementation, Comput. Methods Appl. Mech. Engrg. 98 (1992) 41–104.

Simo, J.C. and K.S. Pister, Remarks on rate constitutive equations for finite deformation problems: computational implicatons, Comput. Methods Appl. Mech. Engrg. 46 (1984) 201–215.

Xiao, H., O.T. Bruhns and A. Meyers, On objective corotational rates and their defining spin tensors, Int. J. solids Struc. 35 (1998) 4001–4014.

Xiao, H., O.T. Bruhns and A. Meyers, Strain rates and material spins, J. Elasticity 52 (1998) 1–41.